Alexandria Engineering Journal (2022) 61, 3747–3756

HOSTED BY

Alexandria University

Alexandria Engineering Journal

www.elsevier.com/locate/aej
www.sciencedirect.com

Synergism analysis in dielectric strength of $CO_2 + N_2 + O_2$ ternary mixtures

M.S. Dincer [a], S.S. Tezcan [b,*], H. Duzkaya [b], S. Dincer [c]

[a] Department of Electrical-Electronic Engineering, Near East University, 99138 Nicosia, Cyprus
[b] Department of Electrical-Electronic Engineering, Gazi University, 06570 Ankara, Turkey
[c] Department of Chemistry, Ankara University, 06100 Ankara, Turkey

Received 23 April 2021; revised 11 July 2021; accepted 24 August 2021
Available online 08 September 2021

KEYWORDS

Electrical discharge;
Electron swarm properties;
Limiting electrical field;
Transport properties

Abstract The synergy effect of O_2 content in dielectric strength of $CO_2 + N_2 + O_2$ ternary mixtures with constant N_2 ratio is investigated from microscopic properties of the component gases. AC Breakdown voltage measurements in the ternary mixtures subjected to uniform electric fields verify the two term Boltzmann equation solutions carried out with the Bolsig + program in the ternary mixtures. The dielectric strength of the ternary mixture increases as the O_2 content is increased and the effect is pronounced at certain fixed N_2 component ratios in the mixtures. The experimental results are valid in the range of 1 cm-bar where the Paschen's Law apply. For the uniform field gap, lightning impulse (LI) voltage breakdown voltages are also measured in the ternary mixtures, however the synergy effect is not significant under the present experimental parameters.

© 2021 THE AUTHORS. Published by Elsevier BV on behalf of Faculty of Engineering, Alexandria University. This is an open access article under the CC BY-NC-ND license (http://creativecommons.org/licenses/by-nc-nd/4.0/).

1. Introduction

SF_6 is widely used in power system components as an insulating and as well as arc-quenching medium. However, it is one of the important greenhouse gases that cause global climate change with a global warming potential (GWP) index of 23.500 times that of CO_2 in a 100-year period [1]. In order to overcome the environmental problems caused by SF_6, the search for alternative non-synthetic and synthetic insulating gases has been going on for about half a century [2,3].

Among non-synthetic alternative gases, CO_2, N_2, O_2, stand out in the literature [3]. These gases, which are abundant in nature, are chemically and thermally stable despite their relatively low dielectric strength compared to SF_6. Noble gases are used as a buffer gas in binary gas mixtures with high dielectric strength such as SF_6. CO_2, N_2 and O_2 can be used in medium-voltage GIS equipment with high-pressure designs [4]. GIS and circuit breakers designed with high pressure CO_2 are commercially operating at voltage levels of 72.5 and 145 kV [5–6].

Although synthetic gases have a very rich variety in the literature, C_4F_7N, $C_5F_{10}O$ and $C_6F_{12}O$ are the most promising alternatives with their very high dielectric strength compared to SF_6 [7–9]. The dielectric strengths of these gases are 2.0–2.7 times higher than that of SF_6. Despite this advantage, higher boiling points of these gases make it a necessity to seek

* Corresponding author.
E-mail address: stezcan@gazi.edu.tr (S.S. Tezcan).
Peer review under responsibility of Faculty of Engineering, Alexandria University.

https://doi.org/10.1016/j.aej.2021.08.080
1110-0168 © 2021 THE AUTHORS. Published by Elsevier BV on behalf of Faculty of Engineering, Alexandria University.
This is an open access article under the CC BY-NC-ND license (http://creativecommons.org/licenses/by-nc-nd/4.0/).

alternative solutions in cold-climate and outdoor GIS applications [10]. CO_2 and N_2 are often used as buffer gases to eliminate this disadvantage in commercial applications of fluoronitriles and ketones [3,7]. These gases examined within the scope of the study also provide useful information for synthetic gas alternative applications.

The relative dielectric strengths of CO_2, N_2 and O_2 gases with respect to SF_6 are 0.44–0.50, 0.37–0.40 and 0.33–0.37, respectively [10]. Despite this relatively low dielectric strength, these non-synthetic alternatives have significant advantages such as low GWP values, lower boiling temperatures, cost and non-toxicity. Although these gases have close dielectric strengths with each other, they have different characteristics in terms of thermal interruption capacity and synergistic effects. For example, CO_2 gas has a better thermal interruption capacity compared to N_2 [11,12].

N_2 gas is one of the most useful alternatives with its zero GWP index as O_2 in the design of environmentally benign green gas insulated switching equipment [3]. Another important advantage of N_2 is that it has many excited states that can slow down free electrons in an avalanche and increase the attachment rate in an electronegative gas mixture thereby controlling the number of free electrons and avalanche growth [13].

In binary and ternary gas mixtures where O_2 is used, it is observed that the insulating property increases by adding O_2 at certain mixture ratios [14,15]. There are significant reductions in the type and amount of decomposition products resulting from electrical discharges in gas mixtures to which O_2 is added [14,15].

This synergistic effect caused by O_2 is also observed in the CO_2-O_2 gas mixture by Zhao *et al* [16]. In this study, a strong synergistic effect is determined in the characteristic of the critical electric field and therefore the breakdown voltage at different concentrations of O_2 in the mixture. The addition of O_2 not only improves the dielectric characteristic of the mixture, but also prevents carbonization and creates a more stable thermally and electrically insulating environment.

This study aims to investigate the synergetic characteristics of the ternary gas mixture of CO_2, N_2 and O_2 gases by using microscopic properties of the component gases together with AC breakdown voltage measurements in the *pd* range (p is the gas pressure and d is the uniform field electrode gap distance) where Paschen's Law is valid. In this context, the calculation method of the synergistic effect of O_2 and the microscopic properties are explained and the detailed experimental procedure for the measurements is given. In the results and discussions, the swarm parameters, namely ionization coefficients, attachment coefficients, limiting electric fields and electron mean energies in the ternary mixtures are given and explained. The critical electric fields calculated with the reduced ionization coefficients and AC breakdown voltage measurements are comparatively defined and the synergistic effect in the ternary gas mixture is investigated. For the sake of completeness Lightning impulse voltage measurements are also carried out in the ternary mixtures with the uniform field electrodes.

2. Synergism and microscopic properties

Synergism is the interaction of two or more agents to produce a total effect, which is greater than the summation of the individual effects of the agents. This nonlinear synergy effect can be calculated by the following empirical formula proposed in a previous paper [17] for the binary gas mixture,

$$V_m = V_2 + \frac{k(V_1 - V_2)}{[k + (1-k)C]} \qquad V_1 > V_2 \tag{1}$$

where V_1, V_2 and V_m are breakdown voltage of pure gases and gas mixture, is the mixing ratio and C is the synergy effect constant. The smaller the C value, the stronger the synergy effect is observed [17]. With the increase of this value, the synergistic effect decreases and the breakdown voltage characteristic between V_1 and V_2 gases changes linearly according to the mixing ratio [18]. The Eq. 1 can be rearranged based on C constant,

$$C = \frac{k(V_1 - V_m)}{(V_m - V_2)(1-k)} = \frac{k_{V1}(V_1 - V_m)}{(V_m - V_2)k_{V2}} \tag{2}$$

where k_{V1} and k_{V1} are the ratio of gases 1 and 2 in the mixture, respectively.

As can be easily seen in Eq. 2, the synergy effect is the ratio of the weighted effects of the gases on the breakdown stress of the mixture. Using this approach, the C constant for $CO_2 + N_2 + O_2$ ternary mixtures can be calculated with the following equation,

$$C = \frac{k_{O2}(V_{O2} - V_m)}{k_{CO2}(V_m - V_{CO2}) + k_{N2}(V_m - V_{N2})} \tag{3}$$

where C constant is the synergy effect of O_2 on the ternary gas mixture. Since the breakdown voltages of these triple gas mixtures arise in the region where the breakdown voltage *pd* characteristic of the Paschen curve changes linearly, Equation 3 can also be written with the number density reduced limiting electric field instead of the breakdown voltage,

$$C = \frac{k_{O2}\left(\frac{E}{N}_{\text{limit O2}} - \frac{E}{N}_{\text{limit m}}\right)}{k_{CO2}\left(\frac{E}{N}_{\text{limit m}} - \frac{E}{N}_{\text{limit CO2}}\right) + k_{N2}\left(\frac{E}{N}_{\text{limit m}} - \frac{E}{N}_{\text{limit N2}}\right)} \tag{4}$$

where the effect is the number density reduced limiting electric field, $(E/N)_{\text{lim}}$, corresponding to the case in which ionization frequency is balanced by attachment frequency in electronegative gas mixtures (E is the applied field magnitude and N is the number density of gas molecules).

3. Calculation of swarm parameters

The ionization and attachment coefficient, mean energy are evaluated in the ternary mixtures using BOLSIG+ [19]. BOLSIG+ is a freeware Boltzmann equation solver to calculate the electron transport coefficients using two-term expansion in a uniform electric field.

The Boltzmann equation for electrons in an ionized gas is

$$\frac{\partial f}{\partial t} + v.\nabla f - \frac{e}{m}E.\nabla_v f = C[f] \tag{5}$$

where f is the electron energy distribution function, v are the velocity coordinates, e and m are electron absolute charge and mass, E is the electric field, ∇_v is the velocity gradient operator and C is rate of change in f.

The electron energy distribution function is symmetric in velocity space around the electric field direction and the electric field and the collision probabilities are all spatially uni-

form. Using the spherical coordinates in velocity space, Eq. 5 can be rewritten as:

$$\frac{\partial f}{\partial t} + v\cos(\theta)\frac{\partial f}{\partial z} - \frac{e}{m}E\left(\cos(\theta)\frac{\partial f}{\partial v} + \frac{\sin^2(\theta)}{v}\frac{\partial f}{\partial \cos(\theta)}\right) = C[f] \tag{6}$$

where θ is the angle between the velocity and the field direction and z is the position along this direction.

To solve the Eq. 6, electron energy distribution function is expanded in terms of Legendre polynomials of $cos(\theta)$. Using the two-term approximation, electron energy distribution function can be expanded as:

$$f(v, \cos(\theta), z, t) = f_0(v, z, t) + f_1(v, z, t)\cos(\theta) \tag{7}$$

where f_0 is the isotropic and f_1 is the anisotropic component. The normalized electron energy distribution function (F_0) is calculated by

$$\int_0^\infty \varepsilon^{0.5} F_0 d\varepsilon = 1 \tag{8}$$

Here, $\varepsilon = \frac{mv^2}{2e}$ and mean energy $(\bar{\varepsilon})$ is calculated by

$$\bar{\varepsilon} = \int_0^\infty \varepsilon^{1.5} F_0 d\varepsilon \tag{9}$$

The reduced Townsend ionization coefficient (α/N) is calculated by

$$(\alpha/N) = \frac{(E/N)(\nu_{iz}/N)}{(P/N)} \tag{10}$$

where (E/N) is reduced electric field, (ν_{iz}/N) is reduced total ionization frequency, (P/N) is energy per unit time absorbed by the electrons from the electric field.

The reduced Townsend attachment coefficient (η/N) is calculated by

$$(\eta/N) = \frac{(E/N)(\nu_{at}/N)}{(P/N)} \tag{11}$$

where (ν_{at}/N) is reduced total attachment frequency.

Total cross-sections of the ternary mixture are taken as the summation of component gas collision cross-sections multiplied by their respective ratios in the mixture in order to set the corresponding cross-section sets. For example the momentum transfer cross section of mixture $(Q_{m\ mix})$is calculated by

$$Q_{m\ mix} = k_{CO2}Q_{m\ CO2} + k_{N2}Q_{m\ N2} + k_{O2}Q_{m\ O2} \tag{12}$$

where (k_{CO2}),$(k_{N2})$and (k_{O2}) define the mixture ratios of the component gases.

In the present paper, the reduced ionization coefficients and the reduced attachment coefficients for constant components of 60 % N_2, 40 % N_2, 20 % N_2 and 10 % N_2 in the mixtures are evaluated as a function of E/N. The limiting electrical field values calculated by Bolsig+ at the specific E/N values where ionization and attachment frequencies are the same. LXCat Siglo, Phelps and Morgan databases are used for collision cross sections of N_2, O_2 and CO_2, respectively [20].

4. Experimental procedure

A stainless steel cylindrical test cell with a height of 300 mm and inner radius of 100 mm is used in the experiments. Two glass viewports of 30 mm diameter and 5 mm thickness are provided to facilitate observation of the electrode arrangement in the test cell. 90° Rogowski profile 35 mm diameter stainless steel electrodes are mounted in a parallel plane configuration. In order to set the electrode gap to a desired value, one of the electrodes is mounted on an isolated mobile platform controlled by a micro-meter providing linear motion. The high voltage bushing of the test cell is a partial discharge free porcelain insulator suitable for measurement of AC and lightning impulse (LI) voltages up to 100 kV. At the high voltage terminal, a sphere terminal with sufficient radius of curvature is available to avoid corona discharges.

To examine the discharge behaviour of the $CO_2+N_2+O_2$ ternary mixtures, the component gases are mixed by adjusting their partial pressure ratios. After evacuating the test cell, to a vacuum pressure of 0.9 Pascal, the lowest component of the mixture is introduced with its corresponding partial pressure. In order to achieve the desired ternary mixture, the component gases are introduced into the test cell from the lowest component ratio to the highest component.

The 50 Hz AC output voltage is measured with a digital voltmeter over the resistive voltage divider. The voltage measurement system has been calibrated in accordance with a standard sphere gap arrangement. At the high voltage terminal of the AC source, a current limiting high voltage resistor is used to avoid pitting and damage electrode surfaces during breakdown voltage tests. The rate-of-rise of the voltage is set at 500 V per second in accordance with the standards [21].

The voltage source used in LI breakdown voltage measurements is an impulse voltage generator that can produce standard impulse voltage. The voltage measurement system of the impulse voltage generator is calibrated in accordance with the standard with a sphere gap arrangement [21]. The breakdown voltage measurements are taken by the up- and down-method, in which the crest voltage is changed at 5% intervals.

The photograph of the experimental setup and its schematic diagram are shown in Figs. 1 and 2, respectively. Before starting a set of experiments for a given ternary mixture, the polished clean electrodes are conditioned as given in Fig. 3.

AC and LI breakdown voltage measurements are taken at 1 bar-10 mm and 2 bar-5 mm conditions in 9 different triple gas mixture samples defined in Table 1.



Fig. 1 Photograph of the experimental setup.

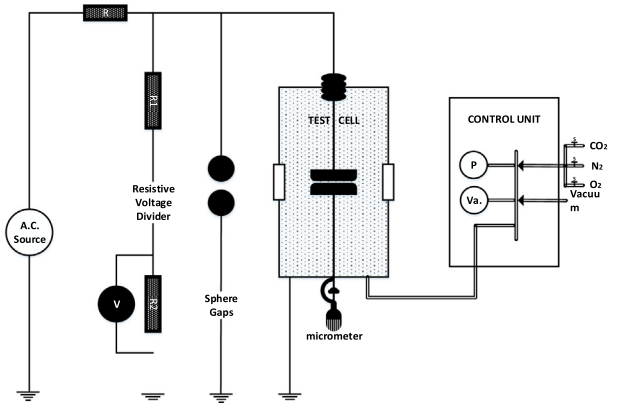


Fig. 2 Schematic diagram of the experimental setup for AC Breakdown voltage measurements.

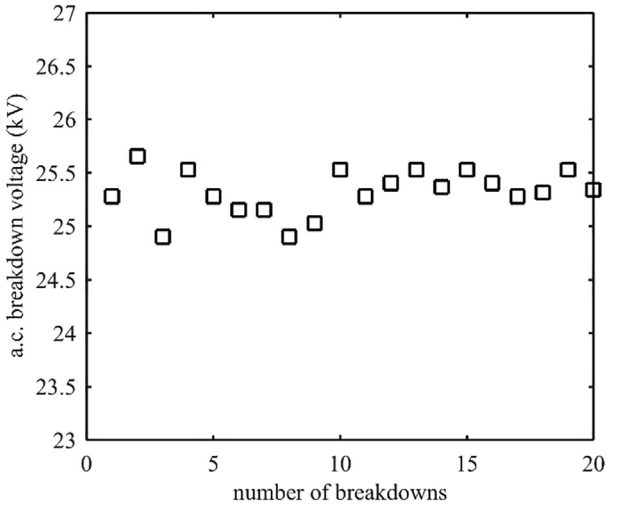


Fig. 3 Conditioning for 45% CO_2 + 40 %N_2 + 15 %O_2 mixture.

Table 1 Gas mixture ratios in breakdown voltage measurements.

Gas mixture sample	CO_2 (%)	N_2 (%)	O_2 (%)
1	60	10	30
2	20	10	70
3	65	20	15
4	50	20	30
5	45	40	15
6	30	40	30
7	10	40	50
8	35	60	5
9	10	60	30

5. Results and discussions

The mean energy in the ternary mixtures is given in Fig. 4 for 10% to 60 % N_2 component. It can be observed from the figures that for the fixed N_2 component in the mixtures, at a given E/N the mean energy drops as the CO_2 concentration is increased. The reduction in mean energy with increasing concentration of CO_2 is due to the increased probability of vibrational excitation collisions of CO_2.

It is interesting to observe from the Fig. 4a, 4b and 4c that, as the N_2 component of the mixture is increased, the mean energy of electrons decreases for the ternary mixtures in the E/N range of the present paper.

The reduction in mean energy at a given E/N is significantly pronounced when the nitrogen component is increased from 10% to 60% concentration in the ternary mixtures. This response of mean electron energy can be seen comparing Fig. 4.a with Fig. 4.d. N_2 is an important buffer gas with its various excited states acting as an energy sink slowing down the energetic electrons [13,22].

In Fig. 5, electron energy distribution functions in binary mixtures of CO_2+N_2 mixtures are shown at the E/N = 100 Td. It can be observed from this figure that the number of slow electrons in the binary mixture increases as the N_2 component in the mixture is increased.

Therefore, when N_2 is mixed with an electronegative gas, due to the increased fraction of slow electrons, it is expected that attachment frequency in the mixture can increase depending on the probability of attachment in the E/N range.

Fig. 6 gives the attachment coefficient in CO_2+N_2 binary mixtures as a function of E/N. It can be observed from this figure that the attachment coefficient in the mixture is higher than that of pure CO_2 for certain mixture ratios depending on E/N. Attachment frequency in 80 % N_2 mixture is higher than that of CO_2 in the E/N range up to 120 Td. Similarly, for E/N values smaller than 105 Td the attachment frequency in 60 % N_2 mixture is higher than that of pure CO_2 and for 40 % N_2 mixture the same response is observed in the E/N interval reaching to about 92 Td.

O_2 is highly electronegative compared to CO_2. Therefore, it is expected that the attachment frequency in CO_2+O_2 binary mixtures will be higher than that of pure CO_2. In Fig. 7, the attachment coefficients in CO_2+O_2 mixtures are shown as a function of E/N. From this figure, it is observed that addition of O_2 increases the attachment frequency in the binary mixture significantly in the E/N range.

The limiting electrical fields calculated in the binary mixtures of CO_2+N_2 and CO_2+O_2 are presented in Fig. 8 together with the swarm experiments reported in the literature [23,24].

The evaluated limiting fields for CO_2 is 77.5 Td which is in agreement with our previous finding [25] and with the results of [16]. The E/N limit in O_2 is evaluated as 126.5 Td with BOLSIG+ that is in good agreement with that of [23]. The critical electrical field for pure nitrogen at breakdown is 118.62 Td [26].

The reduced ionization coefficients and the reduced attachment coefficients for constant N_2 ratios in ternary mixtures in 10%, 20%, 40% and 60 % N_2 concentrations are given respectively, in Fig. 9. The insets in the figures display the crossover points of attachment and ionization coefficients in order to evaluate corresponding E/N limits as the O_2 content in the ternary mixture increases. Reduced ionization coefficients in ternary mixtures decrease with increasing N_2 contents. Ternary mixtures with higher constant N_2 ratios yield reduced ionization coefficients.

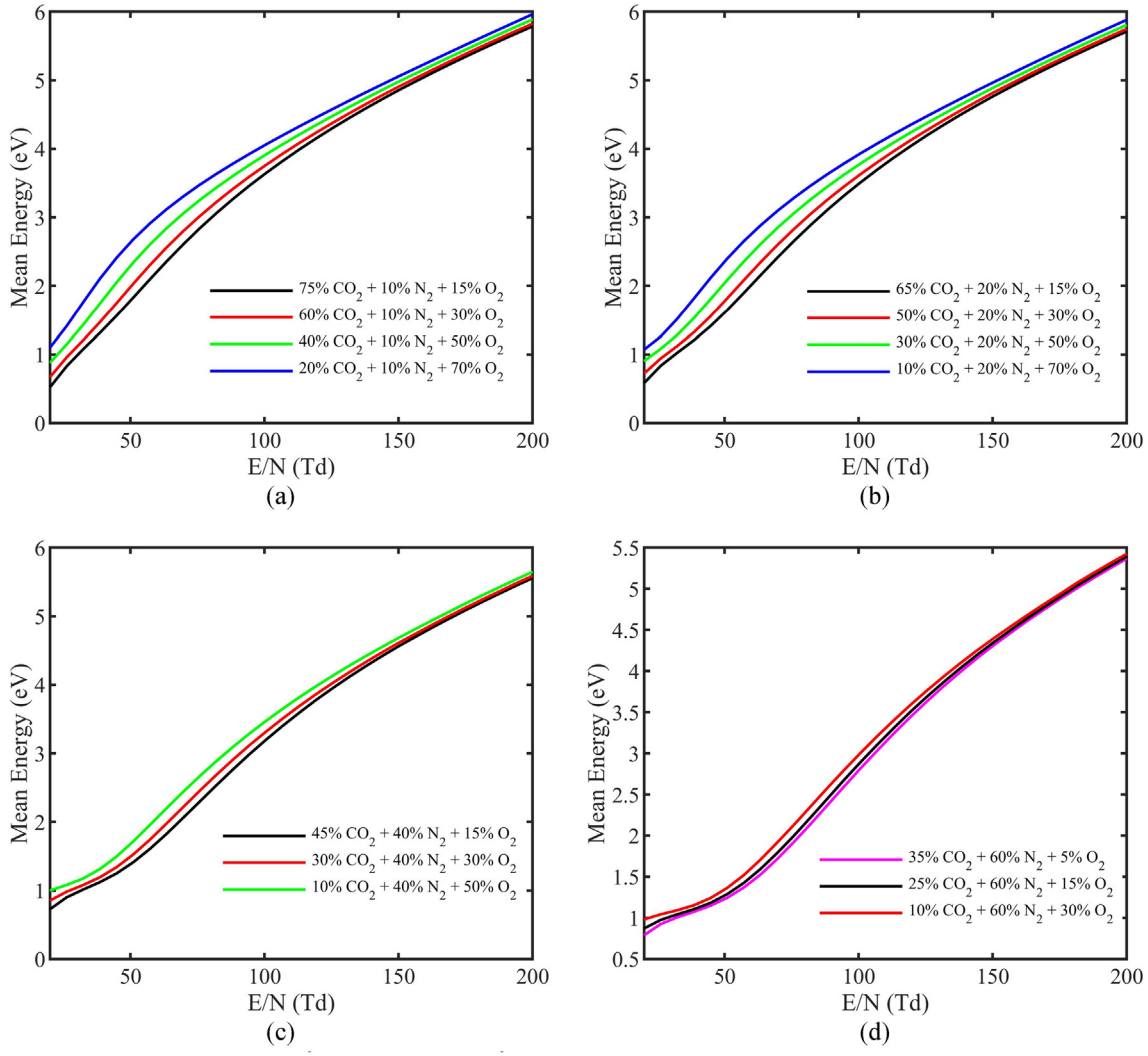


Fig. 4 Mean energies of ternary mixtures for constant N_2: **(a)** %10 N_2, **(b)** %20 N_2, **(c)** % 40 N_2, **(d)** %60 N_2.

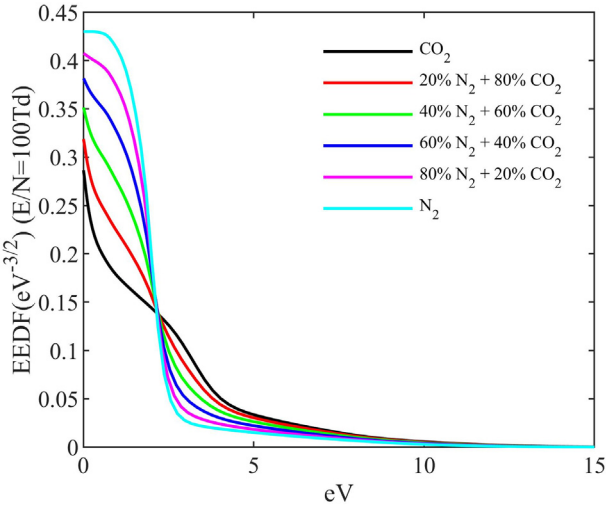


Fig. 5 Electron energy distribution functions in $CO_2 + N_2$ binary mixtures at E/N = 100 Td.

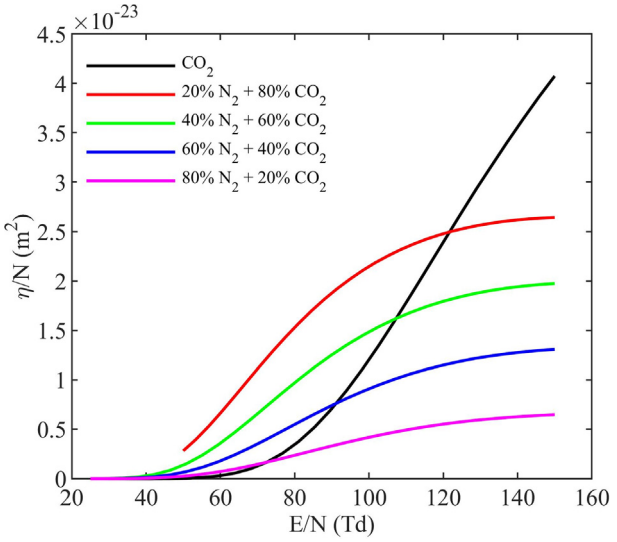


Fig. 6 Attachment coefficient in $CO_2 + N_2$ binary mixtures.

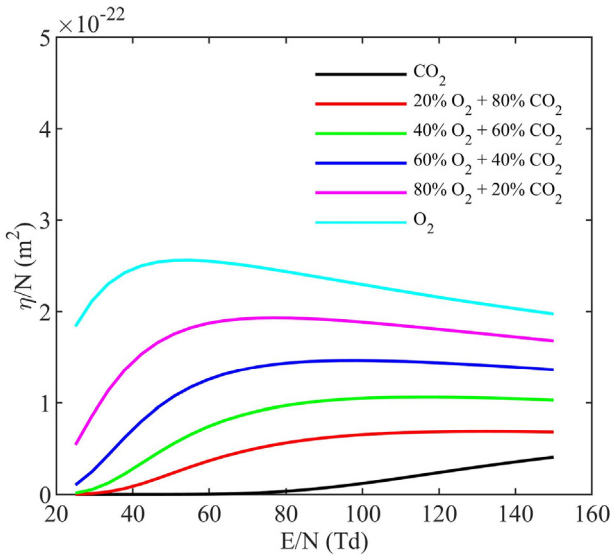


Fig. 7 Attachment coefficient in CO_2+O_2 binary mixtures.

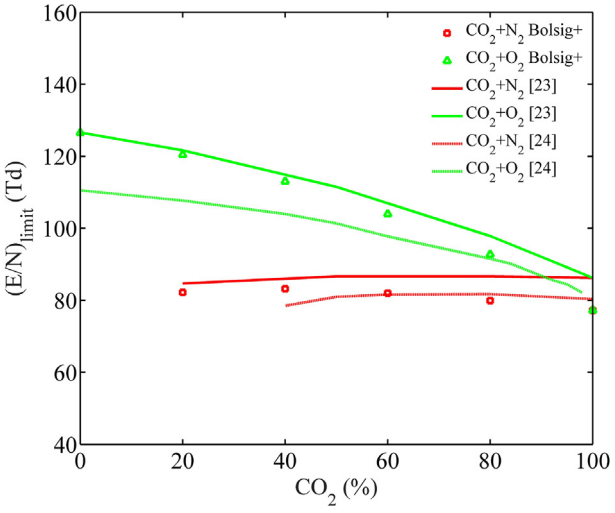


Fig. 8 The limiting electrical fields calculated in CO_2+N_2 and CO_2+O_2 binary mixtures.

For a given ternary mixture of constant N_2 content, the attachment frequency increases with increasing concentration of O_2 resulting in increased dielectric strength. The insets in the figures give the corresponding E/N limit in the ternary mixtures in which ionization coefficient is equal to the attachment coefficient. Furthermore, as the constant N_2 component, concentration is increased, the synergic effect of O_2 component is more pronounced in the related ternary mixtures. Table 2 gives the limiting E/N values in the ternary mixtures for constant N_2 components. In Fig. 10, limiting values of E/N are plotted at constant N_2 components as a function of increasing O_2 content.

In order to relate microscopic properties to macroscopic data, with the experimental system defined, breakdown voltage measurements are conducted with uniform field electrodes in the pd range (p is the gas pressure and d is the gap setting) where Paschen's law is valid. Therefore, it is possible to calculate the limiting E/N from experimental breakdown data using,

$$V_{bd} = (E/p)_{\lim} pd \tag{12}$$

where V_{bd} is the measured breakdown voltage in volts, $(E/p)_{\lim}$ is in $V/cm^{-1}torr^{-1}$ and d is in cm. Therefore $(E/N)_{\lim}$ in Td, is readily defined as

$$\left(\frac{E}{N}\right)_{\lim} = 3.03\frac{V_b}{pd} \tag{13}$$

Table 3 compares the experimental E/N limits with those of theoretical ones in the experimental range of the present study. From the tabulated values, it can be seen that in the ternary mixtures investigated the agreement between theoretical and experimental results is very good. AC breakdown voltages at a given pd product is the average of 5 measurements corresponding to a specific ternary mixture. The standard deviation (σ) and absolute percentage error in the measurements are given in the last two columns.

The agreement between the measurements and the calculations allows us to calculate the synergistic effect of O_2 in the ternary mixture using Eq. 4, see Table 4. $(E/N)_{\lim}$ values for pure O_2, CO_2 and N_2 gases are used 126.47 Td, 77.5 Td and 118.62 Td, respectively, in Eq. 4. Since these limit electric field values calculated for pure gases and mixture are very close to each other, the C constant can be observed outside the values of 0 and 1 as defined in the literature. Negative C constant mean negative synergy. In other words, when the critical electric field value of the gas mixture is compared to pure gases, it exhibits a nonlinear behaviour in the negative aspect. Since there is an inverse proportion between the synergistic effect and the C constant, in order to describe this effect more clearly, the inverse of the C constant is added to the Table 4. This variable, defined as the inverse of the C constant, is used to explain the synergistic effect of O_2 in the mixture, and Fig. 11 is drawn according to this value.

Negative synergy is observed in samples with 5% and 15% O_2 gas in 60 % N_2 mixtures. Since this reduces the limit electric field value of the mixture, alternatives with 20% and 40 % N_2 should be considered for a better insulating gas mixture.

From Fig. 11, the degree of synergy can be observed. In the ternary mixtures with constant N_2 component, synergy effect increases with the increased concentrations of O_2 due to the increased attachment frequencies in the mixtures investigated. Furthermore, synergy effect is more pronounced when the constant N_2 component is increased. O_2 has the highest dielectric strength compared to those of N_2 and CO_2. However, it can also be seen from the Fig. 11 that it is possible to achieve the dielectric strength almost the same as that of pure O_2 in 20% and %40 N_2 ternary mixture with %70 and 50% O_2 concentrations, respectively. N_2 component with its excited states can slow down the energetic electrons in the swarm and slow electrons in the energy range of attachment processes are removed by attachment collisions resulting in higher degrees of synergy.

Another important breakdown voltage characteristic that is considered together with the AC breakdown voltage in the design of gas-insulated systems is lightning impulse (LI). The LI breakdown voltages are measured by using an impulse voltage generator that produces a 1.2/50 μs standard impulse voltage as the voltage source in the experimental setup. LI breakdown voltage measurements are given in Table 5 under the pressure, electrode opening and gas mixture conditions where the AC breakdown voltage is measured.

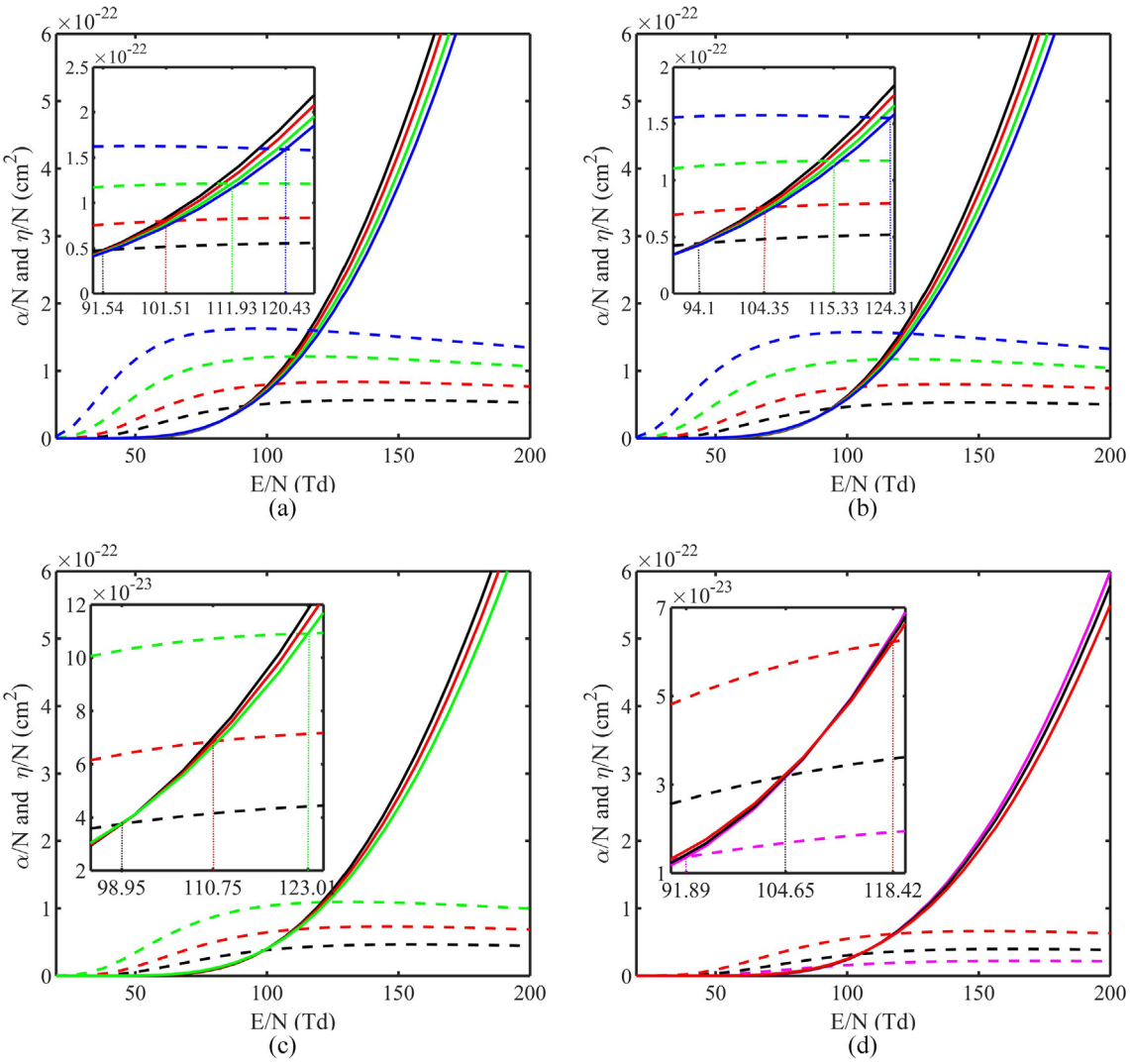


Fig. 9 The reduced ionization coefficients (solid lines) and the reduced attachment coefficients (dashed lines) for constant N_2. The same colours are used for the same mixture ratios as in Fig. 4.

Table 2 The limiting electrical fields calculated by Bolsig+.

CO_2 (%)	N_2 (%)	O_2 (%)	$(E/N)_{lim}$(Td)
75	10	15	91.54
60	10	30	101.51
40	10	50	111.93
20	10	70	120.43
65	20	15	94.10
50	20	30	104.35
30	20	50	115.33
10	20	70	124.31
45	40	15	98.95
30	40	30	110.75
10	40	50	123.01
35	60	5	91.89
25	60	15	104.65
10	60	30	118.42

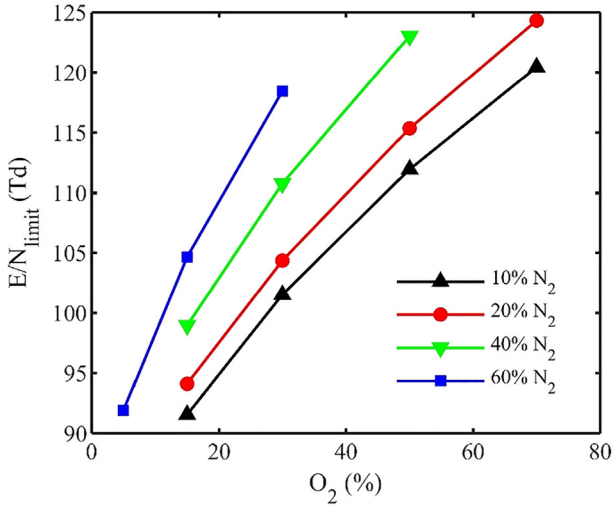


Fig. 10 Limiting electrical field values.

Table 3 The limiting values of E/N, calculated and measured AC breakdown values for special condition of 10 mm-bar in $CO_2+N_2+O_2$ mixture.

p	d	CO_2	N_2	O_2	$(E/N)_{lim}$ with Boltzmann Analysis	$(E/N)_{lim}$ with measured	V_s	σ	PE
(bar)	(mm)	(%)	(%)	(%)	(Td)	(Td)	(kV)	(kV)	(%)
1	10	60	10	30	101.51	99.98	24.75	±1.03	1.51
2	5	60	10	30	101.51	97.27	24.08	±0.63	4.18
1	10	20	10	70	120.43	121.80	30.15	±0.91	1.14
2	5	20	10	70	120.43	115.23	28.52	±0.59	4.32
1	10	65	20	15	94.10	98.19	24.31	±0.61	4.35
2	5	65	20	15	94.10	89.45	22.14	±0.77	4.94
1	10	50	20	30	104.35	107.32	26.57	±0.11	2.85
2	5	50	20	30	104.35	102.88	25.47	±1.72	1.41
1	10	45	40	15	98.95	103.10	25.52	±0.35	4.19
2	5	45	40	15	98.95	102.12	25.28	±0.13	3.21
1	10	30	40	30	110.75	111.17	27.52	±0.55	0.38
2	5	30	40	30	110.75	108.45	26.85	±0.77	2.07
1	10	10	40	50	123.01	123.10	30.47	±1.56	0.07
2	5	10	40	50	123.01	119.72	29.64	±0.48	2.64
1	10	35	60	5	91.89	90.85	22.49	±0.32	1.14
2	5	35	60	5	91.89	92.62	22.93	±0.87	0.79
1	10	10	60	30	118.42	122.15	30.24	±1.10	3.15
2	5	10	60	30	118.42	120.10	29.73	±0.96	1.42

Table 4 The synergetic effect of O_2 in the ternary mixture.

CO_2 (%)	N_2 (%)	O_2 (%)	C	$1/C$
75	10	15	0.6570	1.5221
60	10	30	0.5843	1.7115
40	10	50	0.5516	1.8130
20	10	70	0.4800	2.0831
65	20	15	0.8073	1.2387
50	20	30	0.6220	1.6078
30	20	50	0.5179	1.9309
10	20	70	0.2595	3.8543
45	40	15	2.2009	0.4544
30	40	30	0.6850	1.4599
10	40	50	0.2730	3.6636
35	60	5	−0.1582	−6.3217
25	60	15	−2.1164	−0.4725
10	60	30	0.6056	1.6511

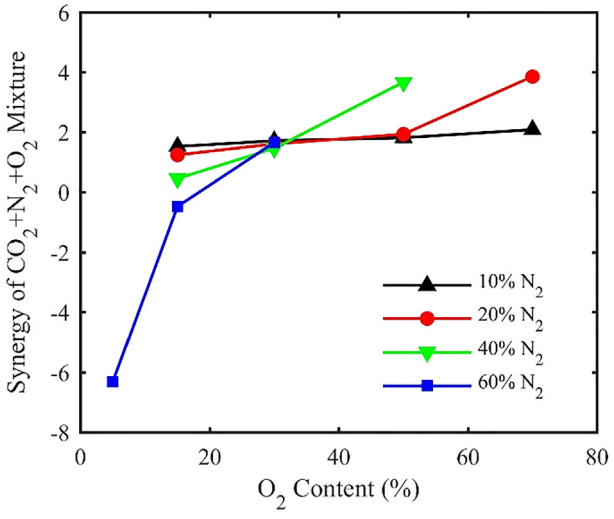


Fig. 11 The synergetic effect of O_2 in the $CO_2+N_2+O_2$ mixtures.

LI breakdown voltage measurements are higher than AC breakdown voltage measurements under the same conditions as observed in the literature [27,28]. While the increase in the O_2 ratio at AC breakdown voltage improves the breakdown voltage characteristic, this effect is limited at the LI breakdown voltage. In the present paper the electrode geometry is symmetrical and produces uniform electric fields since our interest is to investigate synergism with respect to microscopic properties in uniform applied fields in the *pd* range where Panchen's Law is valid. However, it would be interesting to investigate the polarity and the space charge field effect using non-uniform field geometry and the authors are considering non-uniform field study as a future research project.

6. Conclusion

The main results of this study, which examines the microscopic properties and synergy effect in the $CO_2+N_2+O_2$ ternary gas mixture, in the E/N range of the present study are as follows:

- The mean energy of electrons decrease as the N_2 content in the ternary mixture increases.
- Number density reduced ionization coefficients in ternary mixtures decrease with the increasing N_2 component.
- For a given ternary mixture of constant N_2 component, the attachment frequency increases with increasing concentration of O_2 resulting in increased dielectric strength.

Table 5 Measured LI breakdown voltages for special condition of 10 mm-bar in $CO_2+N_2+O_2$ mixture.

p (bar)	*d* (mm)	CO_2 (%)	N_2 (%)	O_2 (%)	V_s (kV)	σ (kV)
1	10	60	10	30	33.94	±0.11
2	5	60	10	30	29.08	±0.24
1	10	20	10	70	32.47	±0.16
2	5	20	10	70	31.14	±0.13
1	10	65	20	15	28.59	±0.25
2	5	65	20	15	27.79	±0.17
1	10	50	20	30	30.58	±0.05
2	5	50	20	30	31.14	±0.18
1	10	45	40	15	30.93	±0.09
2	5	45	40	15	30.51	±0.17
1	10	30	40	30	32.47	±0.12
2	5	30	40	30	31.28	±0.09
1	10	10	40	50	33.03	±0.11
2	5	10	40	50	31.91	±0.11
1	10	35	60	5	31.14	±0.11
2	5	35	60	5	30.51	±0.05
1	10	10	60	30	32.12	±0.16
2	5	10	60	30	31.77	±0.16

- Since O_2 is a more electronegative than CO_2, the attachment frequency and AC breakdown voltage in the mixture increase with the addition of the O_2 in the mixture. This characteristic behavior is confirmed by the limit electric field calculated using electron swarm parameters at the critical E/N value in which attachment frequency is equal to ionization frequency and also validated by breakdown voltage measurements at different pressures and electrode ranges in the experimental parameter range where Pashen's Law apply.
- The synergy effect of O_2 is more dominant in mixtures with 20% and 40 % N_2 contents. In these mixtures, the synergy effect and the breakdown voltage of the mixture increase depending on the increased ratio of O_2. The strong synergy effect is observed in 10 $\%CO_2+\%20$ $N_2+\%70O_2$ and 10 $\%CO_2+\%40$ $N_2+\%50O_2$ mixtures among the ternary mixtures studied.
- This ternary gas mixture offers a potential alternative to the search for environmentally friendly insulating gas in power systems. The calculated and measured breakdown voltage findings show that the $CO_2+N_2+O_2$ gas mixture can be used in medium-voltage equipment as an insulant without degrading the insulation level compared to CO_2 and N_2 only insulated systems.
- In addition to the synergy effect, O_2 gas has the potential to reduce toxic and/or corrosive decomposition products, which are one of the important problems in power system equipment, by chemical reaction mechanisms. This ternary gas mixture also offers the opportunity to prevent the carbonization problem caused by CO_2.
- The lightning impulse breakdown voltages of the mixtures are also measured in the same experimental conditions. With the change of gas ratios in the mixtures, no significant change of breakdown voltage and synergy effect is observed in the measurements. However, the response of the ternary mixture subjected to non-uniform fields should be investigated in order to examine the polarity and space charge field effects which will be the future project of the authors.

Declaration of Competing Interest

The authors declare that they have no known competing financial interests or personal relationships that could have appeared to influence the work reported in this paper.

References

[1] IPCC, 2014: Climate Change 2014: Synthesis Report. Contribution of Working Groups I, II and III to the Fifth Assessment Report of the Intergovernmental Panel on Climate Change [Core Writing Team, R.K. Pachauri and L.A. Meyer (eds.)], IPCC, Geneva, Switzerland, (2015).

[2] Y. Wang, D. Huang, J. Liu, Y. Zhang, L. Zeng, Alternative Environmentally Friendly Insulating Gases for SF_6, Processes 7 (2019) 216, https://doi.org/10.3390/pr7040216.

[3] X. Li, H.u. Zhao, A.B. Murphy, SF_6-alternative gases for application in gas-insulated switchgear, J. Phys. D Appl. Phys. 51 (15) (2018) 153001, https://doi.org/10.1088/1361-6463/aab314.

[4] H. Goshima, S. Okabe, T. Ueda, H. Morii, N. Yamachi, et al, Fundamental insulation characteristics of high-pressure CO_2 gas for gas-insulated power equipment - effect of coating conductor on insulation performance and effect of decomposition products on creeping insulation of space, IEEE Trans. Dielectr. Electr. Insul. 15 (2008) 1023–1030, https://doi.org/10.1109/TDEI.2008.4591223.

[5] ABB, High voltage CO2 Circuit Breaker Type LTA Enhancing Eco-efficiency, (2014).

[6] M. Seeger, Future perspectives on high voltage circuit breaker research, Plasma Sci. Technol 2 (2015) 271.

[7] Y.i. Li, X. Zhang, J.i. Zhang, H. Cui, Y. Zhang, D. Chen, S. Xiao, J.u. Tang, Thermal Decomposition Properties of Fluoronitriles-N_2 Gas Mixture as Alternative Gas for SF_6, J. Fluor. Chem. 229 (2020) 109434, https://doi.org/10.1016/j.jfluchem.2019.109434.

[8] Y.i. Wu, C. Wang, H. Sun, M. Rong, A.B. Murphy, T. Li, J. Zhong, Z. Chen, F. Yang, C. Niu, Evaluation of SF_6-alternative Gas C5-PFK Based on Arc Extinguishing Performance and Electric Strength, J. Phys. D Appl. Phys. 50 (38) (2017) 385202, https://doi.org/10.1088/1361-6463/aa800b.

[9] X. Zhang, S. Tian, S. Xiao, Z. Deng, Y. Li, J. Tang, Insulation Strength and Decomposition Characteristics of a $C_6F_{12}O$ and N_2 Gas Mixture, Energies 10 (2017) 1170, https://doi.org/10.3390/en10081170.

[10] H. Duzkaya, S.S. Tezcan, A. Acarturk, M. Yilmaz, Environmental and Physiochemical Properties of Gaseous Dielectrics Alternatives to SF_6, El-Cezerî Journal of Science and Engineering 7 (2020) 1460–1470, https://doi.org/10.31202/ecjse.742492.

[11] P.C. Stoller, M. Seeger, A.A. Iordanidis, G.V. Naidis, CO_2 as an Arc Interruption Medium in Gas Circuit Breakers, IEEE Trans. Plasma Sci. 41 (2013) 2359–2369, https://doi.org/10.1109/TPS.2013.2259183.

[12] T. Uchii, Y. Hoshina, T. Mori, H. Kawano, T. Nakamoto, H. Mizoguchi, in: Gaseous Dielectrics X, Springer US, Boston, MA, 2004, pp. 205–210, https://doi.org/10.1007/978-1-4419-8979-6_28.

[13] M.S. Dincer, S.S. Tezcan, H. Duzkaya, Suppression of Electron Avalanches in Ultra-Dilute SF_6-N_2 Mixtures Subjected to Time-Invariant Crossed Fields, Energies 11 (2018) 3247, https://doi.org/10.3390/en11123247.

[14] Y. Li, X. Zhang, F. Ye, D. Chen, S. Tian, Z. Cui, Influence Regularity of O_2 on Dielectric and Decomposition Properties of C_4F_7N-CO_2-O_2 Gas Mixture for Medium-Voltage Equipment, IET High Volt. 5 (3) (2020) 256–263, https://doi.org/10.1049/hve2.v5.310.1049/hve.2019.0219.

[15] Y. Li, X. Zhang, Q. Chen, J. Zhang, Y. Li, S. Xiao, J. Tang, Influence of Oxygen on Dielectric and Decomposition Properties of C_4F_7N-N_2-O_2 Mixture, IEEE Trans. Dielectr. Electr. Insul. 26 (4) (2019) 1279–1286, https://doi.org/10.1109/TDEI.9410.1109/TDEI.2019.007996.

[16] H.u. Zhao, Y. Deng, H. Lin, Study of the synergistic effect in dielectric breakdown property of CO_2–O_2 mixtures, AIP Adv. 7 (9) (2017) 095102, https://doi.org/10.1063/1.4996357.

[17] O. Yamamoto, T. Takuma, S. Hamada, Y. Yamakawa, M. Yashima, Applying a gas mixture containing c-C_4F_8 as an insulation medium, IEEE Trans. Dielectr. Electr. Insul. 8 (2001) 1075–1081, https://doi.org/10.1109/94.971467.

[18] Y. Wang, J.Q. Liang, C.L. Yu, L. Li, H.D. Zhang, G.X. Li, Research on the synergy of SF6/N2 mixture gas in low temperature environment, IOP Conf. Series: Materials Science and Engineering 479 (2019) 012045, https://doi.org/10.1088/1757-899X/479/1/012045.

[19] G.J.M. Hagelaar, L.C. Pitchford, Solving the Boltzmann equation to obtain electron transport coefficients and rate coefficients for fluid models, Plasma Sources Sci. Technol. 14 (4) (2005) 722–733, https://doi.org/10.1088/0963-0252/14/4/011.

[20] L.C. Pitchford, L.L. Alves, K. Bartschat, S.F. Biagi, M.C. Bordage, et al, LXCat: an Open-Access, Web-Based Platform for Data Needed for Modelling Low Temperature Plasmas, Plasma Process. Polym. 14 (2017) 1600098, https://doi.org/10.1002/ppap.201600098.

[21] High-voltage test techniques - Part 1: General definitions and test requirements, IEC Standard 60060-1 ed3.0, (2010).

[22] M.S. Dincer, O.C. Ozerdem, S. Bektas, Effective Ionization Coefficients and Transport Parameters in Ultradilute $SF_6 + N_2$ Mixtures, IEEE Trans. Plasma Sci. 35 (2007) 1210–1214, https://doi.org/10.1109/TPS.2007.905205.

[23] M. Yousfi, J. de Urquijo, A. Juarez, E. Basurto, J.L. Hernandez-Avila, Electron Swarm Coefficients in CO_2-N_2 and CO_2-O_2 Mixtures, IEEE Trans. Plasma Sci. 37 (2009) 764–772, https://doi.org/10.1109/TPS.2009.2017538.

[24] P. Haefliger, C.M. Franck, Comparison of swarm and breakdown data in mixtures of nitrogen, carbon dioxide, argon and oxygen, J. Phys. D Appl. Phys. 52 (2) (2019) 025204, https://doi.org/10.1088/1361-6463/aae60f.

[25] M.S. Dincer, S.S. Tezcan, H. Duzkaya, S. Dincer, Determination of Electron Swarm Parameters and Limiting Electrical Field during Martian Dust Storm Season Using Boltzmann Analysis, Acta Phys. Pol. A 138 (2020) 368–376, https://doi.org/10.12693/APhysPolA.138.368.

[26] H. Fujita, T. Kouno, Y. Noguchi, S. Ueguri, Breakdown voltages of gaseous N_2 and air from normal to cryogenic temperatures, Cryogenics 18 (4) (1978) 195–200, https://doi.org/10.1016/0011-2275(78)90001-2.

[27] A. Beroual, M. Coulibaly, Experimental investigation of breakdown voltage of CO2, N2 and SF6 gases, and CO2-SF6 and N2-SF6 mixtures under different voltage waveforms, 2016 IEEE IPMHVC, San Francisco, CA, (2016) 292-295, https://doi.org/10.1109/IPMHVC.2016.8012898.

[28] A. Beroual, U. Khaled, M. Coulibaly, Experimental Investigation of the Breakdown Voltage of CO_2, N_2, and SF_6 Gases, and CO_2–SF_6 and N_2–SF_6 Mixtures under Different Voltage Waveforms, Energies 11 (2018) 902, https://doi.org/10.3390/en11040902.